

TOWARD QUANTITATIVE X-RAY CT PHANTOMS OF METASTATIC TUMORS USING RAPID PROTOTYPING TECHNOLOGY

Terry S. Yoo¹, Trevor Hamilton¹, Darrell E. Hurt², Jesus Caban¹, David Liao¹, David T. Chen¹

¹Office of High Performance Computing and Communications, NLM, NIH, Bethesda, MD

²Office of Cyber Infrastructure and Computational Biology NIAID, NIH, Bethesda, MD

ABSTRACT

We are seeking ground-truth 3D X-ray CT phantoms with gradations of Hounsfield units that are indistinguishable from scans of human subjects. We modified a 3D printer, a ZCorp Spectrum 510, adding an iodine-based contrast agent, and printed physical models using a powder which consists mainly of cellulose and cornstarch. We scanned these 3D models with a Siemens Somatom Definition AS 128-slice CT scanner. By adjusting the level of iodine within the model, we are able to achieve Hounsfield units as high as 1056, mimicking bone, and as low as -450, similar to pulmonary tissue. We demonstrate how to generate grayscale images within a 3D model that can be imaged using a CT scanner. Unlike solid tumor phantoms, these models can accurately mimic lesions with indistinct boundaries similar to metastatic disease. Our intent is to evaluate the accuracy of computer aided diagnosis systems.

Index Terms—Tomographic imaging, Computational imaging, X-ray imaging, Three-dimensional image acquisition.

1. INTRODUCTION

Evaluation and validation of segmentation algorithms remains an elusive but important problem, especially in the context of measuring pathogenesis, the growth, reduction, or change of a lesion, infection, cyst, or tumor. Oncologists and radiologists have debated the merits of imaging as a biomarker, measuring changes in tumor volume sizes from medical images as a means of measuring response to treatment [2, 8, 9]. One impediment to advances in this research is the relative lack of quantitative studies for accurately and repeatedly making precise calculations of tumor size and being able to compare these results to known ground truth.

Using computer aided manufacturing, we can reproduce inert devices accurately that have repeatable shape and internal structure. Commercial 2D X-ray calibration phantoms are frequently used to perform routine maintenance on medical scanners. Heretofore most work on anthropomorphic and clinical phantoms has been limited to solid structures with distinct boundaries. We are working toward

the manufacturing of reproducible 3D phantoms for x-ray CT imaging that can mimic both solid tumors as well as metastatic disease with soft boundaries. We intend for these soft boundaries to be mathematically quantifiable, allowing us to precisely determine the extent and accuracy of tumor detection and analysis by computer-aided diagnosis tools.

2. BACKGROUND AND RELATED WORK

The clinically accepted metric for assessing tumor size is the RECIST criteria, a linear measurement across the longest axis of the lesion taken from a single slice of a CT scan [3, 13]. The tacit assumption in this metric is that this single dimension can determine volume, implying that all tumors are spherical in shape and that the radius of the lesion can be measured accurately from one cross-section [6]. More robust methods have been studied to measure tumor volume, but reproducible results are subject to the control of a variety of factors including the methodology of the segmentation and classification algorithms [4].

To enable quantitative, repeatable analysis across institutions and algorithms, phantoms with known lesion sizes, shapes, and positions are used to provide ground truth and to enable the acquisition of multiple scans to compare imaging from different models and manufacturers of imaging equipment, not possible with human subjects because of the unnecessary additional radiation exposure [9]. Levine, *et al.*, use rapid prototyping methods to create measured ellipsoidal shapes for a test phantom to illuminate some of the shortcomings of the RECIST criteria [10]. Recent work by Gavrielides, *et al.*, in tumor measurement also featured rapid prototyping techniques; however, their work included artificial nodules with complex shapes embedded in an anthropomorphic chest phantom that better represents the problem posed by real clinical pathologies [5]. The use of anthropomorphic models is not limited to lung anatomy; Birnbaum, *et al.*, studied the imaging of renal cysts using a body CT phantom [1].

Aside from our work presented here, other research teams have used printing technology to adjust contrast or include other imaging agents in the production of phantoms. Kotre and Porter used laser printers and mylar sheets to produce 2D mammography calibration phantoms, relying on the iron oxide content of the toner to create differential x-ray

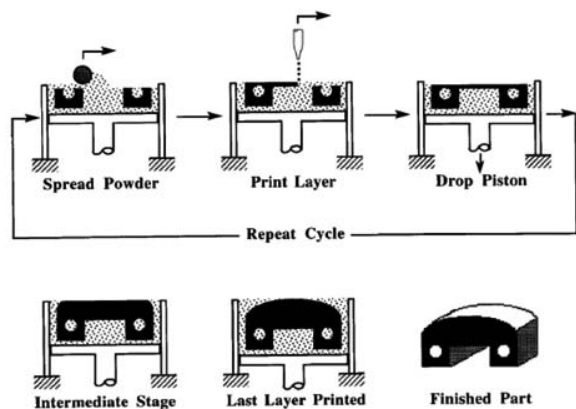


Figure 1. Schematic of the 3D Printing process. Layers of powder are deposited and fused in a controlled manner with a liquid binder using an inkjet head [15]. We use a powder consisting mostly of cellulose and cornstarch. We amend the liquid binder with NaI to selectively add x-ray contrast to the part.

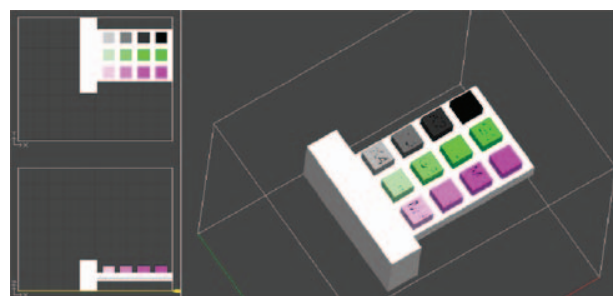
contrast [7]. Miller and Hutchins independently conceived and performed the work that is closest to that presented here, adjusting the chemistry of a ZCorp printer with radioisotopes created with a cyclotron to generate 3D models that can be resolved using a PET scanner. They also conjecture about the development of modified powders for the production of phantoms or the development of new inkjet pigments with massive additives such as bismuth nano-particles to achieve higher contrast [11].

Our research directions differ from the previous studies by incorporating smooth gradients and soft edges to the parts and simulated lesions that can realistically portray metastatic tumors. We independently conceived these ideas, and though our ideas converged on the same technology as Miller and Hutchins, rather than adding heavy metals to our chemistry, we pursued more conventional x-ray contrast elements such as iodine and took these ideas beyond conjecture and have run preliminary tests demonstrating their potential.

3. THREE-D PRINTING WITH CONTRAST

Three-D printing is a rapid prototyping technology originally introduced in the early 1990s. Developed at MIT, 3D printing falls in the family of layered manufacturing methods that feature the controlled addition of material and fused using an inkjet head and a liquid binder [12]. Figure 1 shows the basic process by which layers are deposited eventually generating a 3D model [15].

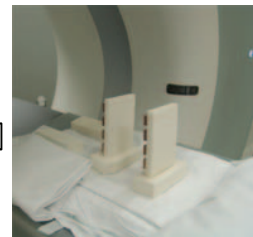
Figure 2 depicts the process by which we created our test models. While multiple powders are available as a build matrix for these models, we specifically chose zp15e. This material contains no calcium and is made with only light organic compounds giving it a low native x-ray



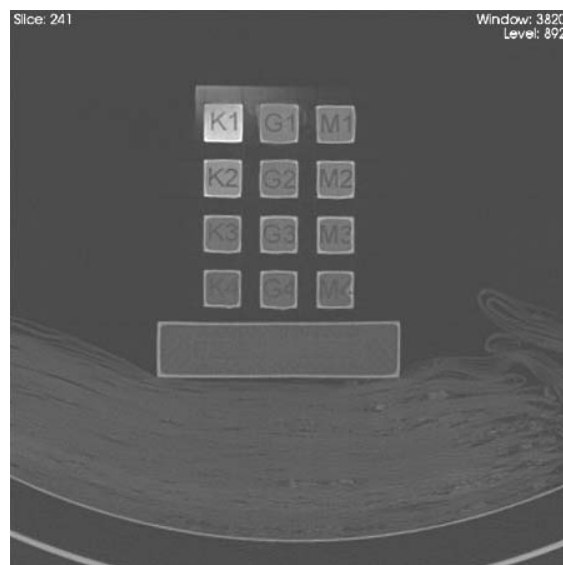
2a. Part layout in ZPrint software



2b. ZCorp 3D printer



2c. Siemens CT scanner



2d. A single slice of the resulting scanned image of the test model.

Figure 2. Fabrication of the contrast test pattern. Layout of the test block is completed on the ZPrint CAD software (2a) and sent to the ZCorp Spectrum 510 printer (2b). The pigmented binder has been amended with NaI at a ratio of 1g NaI / 1 ml of fluid. The resulting models are imaged in a CT scanner (2c). The resulting object has differing xray attenuation properties depending on the concentration of the amended binder in that volume (2d).

attenuation coefficient suitable for modeling tissues with the same density as water or lower.

We begin with the standard binder for the selected powder, zb58, mostly consisting of glycol and water, but we amended the liquid with high concentrations of sodium iodide (NaI). By trial and error and multiple tests, we concluded that a 1:1 ratio by mass of 1g NaI to 1 ml of zb58

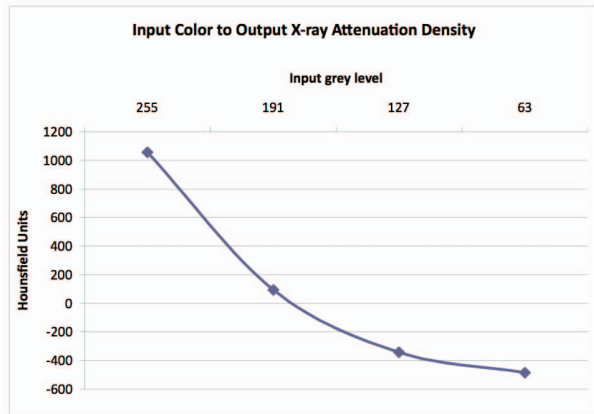


Figure 3. X-ray attenuation values corresponding to input grey values for the 3D printer. The plot is approximately linear with a range from 1000 H.U. (bone) to -480 H.U. (lung), enabling smooth and relatively predictable rendering of complex information.

would yield the desired results without clogging the inkjet heads. The chemistry of the pigmented binder liquids prevents us from creating colored parts. The 3D printer uses three pigmented binders: cyan, yellow, and magenta. NaI interacts adversely with the yellow and magenta binder, precipitating the pigments out of suspension and making them unsuitable for printing.

We designed a test model with twelve blocks each of constant contrast to help measure the amount of amended binder needed to achieve a specific measured Hounsfield unit. We deeply debossed alphanumeric characters to easily identify each block no matter what slice we selected from the resulting CT scan. The rows and columns were designated to map the CMY color space to test the linearity of the x-ray contrast printout. The magenta column of blocks uses only one of the inkjet heads, the green column combines the cyan and yellow inkjet heads, and the grey column uses all three heads. A fourth print head used only for binding to build without pigment (or contrast in our case) was left as native zb58 with no added NaI.

5. TEST PATTERN RESULTS

We scanned the test pattern with an abdominal protocol, 120 kVP, 512x512, 1mm slices, on a Siemens Somatom Definition AS 128-slice CT scanner (Fig. 2c). Table 1 summarizes the results of the test pattern experiment listing the Hounsfield units achieved with different color values sent to the printer. Analysis of the density of each of the shaded squares shows the best results were achieved when printing with all three inkjet heads combined, corresponding to the grayscale colors of the CMY color space.

By convention, Housfield units are normalized so that bone has a density of 1000, water is 0, and air is -1000. Our experiment showed that we are able to achieve values equivalent to bone and approaching air in our models. Moreover, the response of output density to input color is nearly linear, enabling predictable color management.

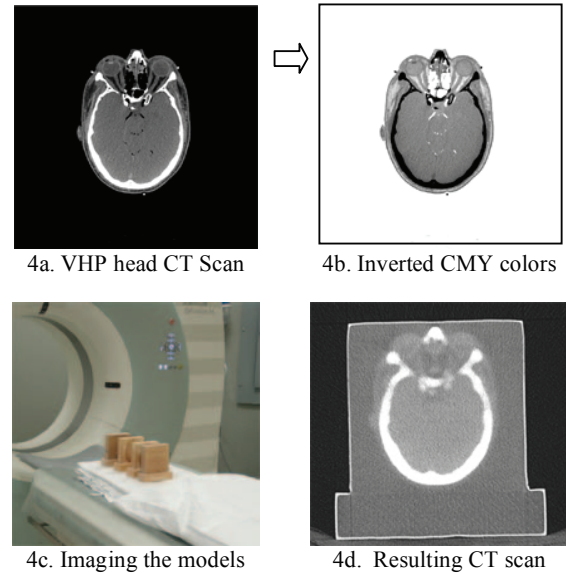


Figure 4. Description and results of the first demonstration case. A slice from a head CT scan (4a) is inverted (4b) and extruded into a 3D model, printed and scanned (4c). The resulting image (4d) clearly shows hard and soft tissue matching the original data.

6. DEMONSTRATIONS

Based on the promising results of our test pattern, we attempted two models to demonstrate the ability to print greyscale gradients inside 3D models. Figure 4a shows a slice from the CT scan from the male data set of the Visible Human Project. We inverted the grey levels (Fig. 4b) and converted them to the corresponding CMY values and embedded them in a 3D model test tablet which we sent to the printer. The models were scanned (Fig. 4c), and the resulting slice data (Fig. 4d) shows the embedded image rendered using an x-ray contrast agent. Both soft and hard tissues are clearly distinguishable in the output image, demonstrating the viability of these methods. Figure 5 shows the results of our second demonstration model.

	Input CMY values	Average Density (Hounsfield Units)	StdDev
material only	(0,0,0)	-631.8199387	16.84
K1	(255,255,255)	1056.448564	36.02
K2	(191,191,191)	92.59012371	20.65
K3	(127,127,127)	-343.1649806	14.19
K4	(63,63,63)	-484.9999983	13.75
G1	(255,0,255)	-160.1921294	22.70
G2	(191,0,191)	-229.2703705	30.25
G3	(127,0,127)	-319.7811465	18.47
G4	(63,0,63)	-434.9228363	13.71
M1	(0,255,0)	-207.674603	16.16
M2	(0,191,0)	-228.4592601	13.64
M3	(0,127,0)	-336.0703715	16.89
M4	(0,63,0)	-454.8866222	17.79

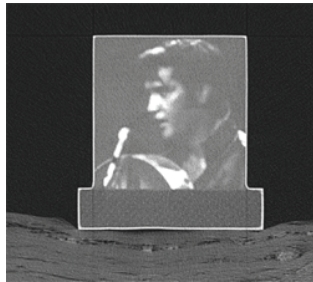
Table 1. Density of the blocks of the test pattern from Fig. 2, standard deviation of each measurement and the input CMY values



5a. A familiar image



5b. Inverted CMY colors



5c. CT slice of the model



5d. Volume rendering

Figure 5. Second demonstration case. A familiar image (5a) is inverted (5b) and extruded into a 3D model, printed and scanned (5c). The transparent volume rendering (5d) shows the 3D nature of how the contrast is deposited through the z-dimension.

8. CONCLUSIONS AND FUTURE WORK

We set out to evaluate the possibility of printing gradient information in the interior of 3D models to enable the generation of CT phantoms for the study of tumors with both hard and soft boundaries. Our study shows that we are clearly capable of printing models with embedded structures resolvable with CT scans. Quantitative models that mimic metastatic disease are within reach.

So far we have shown 2D images that have been extruded into 3D. We require a 3D test pattern and a better API for communicating with the printer. Our successful 2½-D tests will be followed by new experiments with more sophisticated analysis on contrast and resolution.

10. ACKNOWLEDGEMENTS

This work was enabled in part by the generous help of the Radiology Department at the Georgetown University School of Medicine, in particular, Emmanuel Wilson and Kevin Cleary of the Georgetown ISIS Center. We are also indebted to the NIH Summer Internship Program for their support of two of our investigators during their brief tenure at NIH.

11. REFERENCES

- [1] B.A. Birnbaum, D.D. Maki, and D.P. Chakraborty, "Renal Cyst Pseudoenhancement: Evaluation with an Anthropomorphic Body CT Phantom," *Radiology*, 2002.
- [2] L.P. Clarke, R.D. Sriram, L.B. Schilling, "Imaging as a biomarker: standards for change measurements in therapy: workshop summary," *Acad Radiol.*, 15(4), pp. 501-530, 2008

- [3] E.A. Eisenhauer, P. Therasse, J. Bogaerts, L.H. Schwartz, D. Sargent, R. Ford, J. Dancey, S. Arbuck, S. Gwyther, M. Mooney, L. Rubinstein, L. Shankar, L. Dodd, R. Kaplan, D. Lacombe, and J. Verweij, "New response evaluation criteria in solid tumours: Revised RECIST guideline (version 1.1)," *European Journal of Cancer*, 45, pp. 228-247, 2009.
- [4] M.A. Gavrielides, L.M. Kinnard, K.J. Myers, and N. Petrick, "Non-calcified lung nodules: Volumetric assessment with thoracic CT," *Radiology*, 251, pp. 1-11, 2009.
- [5] M.A. Gavrielides, L.M. Kinnard, K.J. Myers, J. Peregoy, W.F. Pritchard, R. Zeng, J. Esparza, J. Karanian, and N. Petrick, "A resource for the development of methodologies for lung nodule size estimation: database of thoracic CT scans of an anthropomorphic phantom," *Optics Express*, 18, Optical Society of America, Washington D.C., pp. 15244-15255, 2010.
- [6] C.C. Jaffe, "Measures of response: RECIST, WHO, and new alternatives," *Journal of Clinical Oncology*, 24, 3245-3251, 2006.
- [7] C.J. Kotre and D.J.T. Porter, "A printed image quality test phantom for mammography," *The British Journal of Radiology*, 78, The British Institute of Radiology, London, 746-748, 2005.
- [8] K. Krishnan, L. Ibanez, W. Turner, and R. Avila, "Algorithms, architecture, validation of an open source toolkit for segmenting CT lung lesions," in *MICCAI Pulmonary Image Analysis Workshop*, pp. 365-375, Sep-2009.
- [9] Z.H. Levine, B.R. Borchardt, N.J. Branderburg, C.W. Clark, B. Muralikrishnan, C.M. Shakarji, J.J. Chen, and E.L. Siegel, "RECIST versus volume measurement in mediastinal CT using ellipsoids of known size," *Optics Express*, 18(8), pp. 8151-8159, 2010.
- [10] C.R. Meyer, S.G. Armato, C.P. Fenimore, G. McLennan, L.M. Bidaut, D.P. Barboriak, M.A. Gavrielides, E.F. Jackson, M.F. McNitt-Gray, P.E. Kinahan, et al., "Quantitative imaging to assess tumor response to therapy: common themes of measurement, truth data, and error sources," *Transl Oncol.* 2(4) pp. 198-210, 2009.
- [11] M.A. Miller and G.D. Hutchins, "Development of anatomically realistic PET and PET/CT phantoms with rapid prototyping technology," in *Proc. IEEE Nuclear Science Symposium*, 6, pp. 4252-4257, 2007.
- [12] E. Sachs, M. Cima, J. Cornie, D. Brancazio, J. Bredt, A. Curodeau, T. Fan, S. Khanuja, A. Lauder, J. Lee and S. Michaels, "Three-dimensional printing: the physics and implications of additive manufacturing," *CIRP Annals - Manufacturing Technology*, 42(1), pp. 257-260, 1993.
- [13] C. Theodorakou, J.A. Horrocks, N.W. Marshall, and R.D. Speller, "A novel method for producing x-ray test objects and phantoms" *Phys Med Biol*, 49, pp. 1423-38, 2004.
- [14] P. Therasse, S. G. Arbuck, E. A. Eisenhauer, J. Wanders, R. S. Kaplan, L. Rubinstein, J. Verweij, M. V. Glabbeke, A. T. v. Oosterom, M. C. Christian, and S. G. Gwyther, "New guidelines to evaluate the response to treatment in solid tumors," *Journal of the National Cancer Institute*, 92, pp. 205-216, 2000.
- [15] P.A. Williams, "Three-dimensional printing: a new process to fabricate prototypes directly from CAD models," Master's thesis, Department of Mechanical Engineering, MIT, 1998.